NATIONAL WATER RESEARCH INSTITUTE

INSTITUT NATIONAL de RECHERCHE sur les EAUX

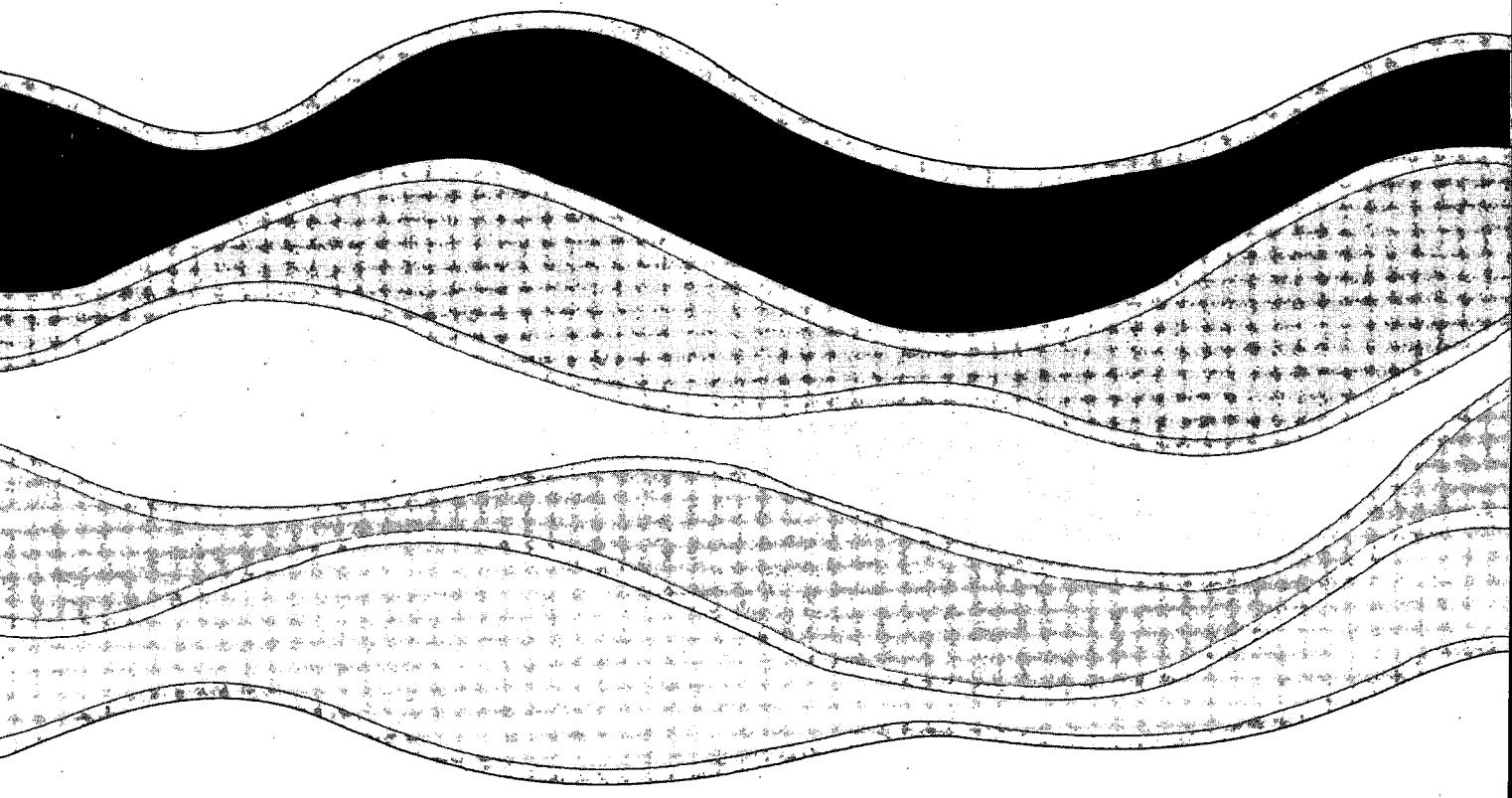

PRELIMINARY TESTS FOR THE ISO-KINETIC CALIBRATION OF THE DH-81 SUSPENDED SEDIMENT SAMPLER

P. Engel and I.G. Droppo

NWRI CONTRIBUTION 90-143

NWRI CONTRIBUTION: 90-143

PRELIMINARY TESTS FOR THE ISO-KINETIC CALIBRATION OF THE DH-81 SUSPENDED SEDIMENT SAMPLER

by

P.Engel[1] and *I.G.Droppo*[2]

1. Hydraulics Studies Project, Research and Applications Branch.
2. Environmental Hydraulics and Large Basin Studies, Rivers Research Branch.

MANAGEMENT PERSPECTIVE

Suspended solids play a strong role in the biological and chemical balance of the aquatic environment. The important components of the suspended load for geochemical transport are silts, clays and organic carbons. These components are also identified as important for the transport of contaminants such as heavy metals, phosphorous and a wide range of synthetic, organic substances, especially where sediment transport is high.

Sediment and water chemistry of small rivers in Ontario are an important component of the research program at the National Water Research Institute. Accurate measurement of suspended solids concentration and distribution in both space and time is critical. All measurements for low to medium flows are made with the US DH-81 suspended sediment sampler. It is known that this instrument oversamples at lower flows and under samples at medium to higher flows. Carefully conducted tests in a towing tank have shown that the sampling performance of this sampler can be significantly improved. The results of this study have wide implications for sediment measurement programs in general.

Dr. J. Lawrence
Director
Research and Applications Branch

PERSPECTIVES DE GESTION

Les matières solides en suspension jouent un grand rôle dans le bilan biologique et chimique de l'environnement aquatique. Les constituants de la charge en suspension, importants pour le transport géochimique, sont les limons, les argiles et les carbones organiques. Ces constituants sont également reconnus comme importants pour le transport de contaminants comme les métaux lourds, le phosphore et une grande gamme de substances organiques synthétiques, surtout là où le transport par les sédiments est considérable.

La chimie des sédiments et de l'eau des petites rivières de l'Ontario représente un élément important du programme de l'Institut national de recherche sur les eaux. Des mesures exactes et précises de la concentration et de la distribution des matières solides en suspension dans le temps et dans l'espace sont d'une importance capitale. Toutes les mesures pour les débits faibles à moyens sont effectuées à l'aide de l'échantillonneur US-DH-81 de sédiments en suspension. On sait que cet instrument sur-échantillonne aux faibles débits et sous-échantillonne aux débits moyens à élevés. Des essais effectués avec soin dans un réservoir de touage ont montré que l'efficacité d'échantillonnage de cet instrument peut être sensiblement améliorée. Les résultats de cette étude ont des répercussions très étendues pour les programmes de mesure des sédiments en général.

J. Lawrence

Directeur

Direction de la recherche et des applications

SUMMARY

Dimensional considerations and detailed tests in a towing tank were used to determine the response of the US DH-81 suspended sediment sampler to flow velocity. The data revealed a clear relationship between sampling rate and the size of the air exhaust port for the operating range of this instrument. It was observed, that the importance of the diameter of the air vent relative to the inside diameter of the intake nozzle decreased as their ratio increased, indicating that there is a transition point between nozzle control and air vent control governing the inflow to the sampler. It was further shown, using dimensional analysis, that a single dimensionless calibration curve can be established which is valid at all water temperatures likely to be encountered during measurements in the field. Further tests are recommended to determine the effect of nozzle diameter on the dimensionless calibration curve and the control regime of the D-77, DH-81 and other samplers used by data gathering agencies.

RÉSUMÉ

Des études dimensionnelles et des essais détaillés dans un réservoir de touage ont servi à déterminer la réponse d'un échantillonneur US DH-81 de sédiments en suspension, à la vitesse du débit. Les résultats ont révélé une relation très nette entre la vitesse d'échantillonnage et la taille de l'orifice d'évacuation pour l'intervalle de fonctionnement de cet instrument. On a constaté que l'importance du diamètre de la prise d'air par rapport au diamètre interne de l'orifice d'admission diminuait à mesure que leur rapport augmentait, ce qui montre qu'il existe un point de transition entre le réglage de l'orifice et celui de la prise d'air, qui détermine le débit d'entrée dans l'échantillonneur. De plus, une analyse dimensionnelle a permis de montrer qu'une courbe d'étalonnage unique sans dimensions peut être obtenue et qu'elle est valable pour toutes les températures de l'eau que l'on peut rencontrer pendant les mesures sur le terrain. D'autres essais sont proposés pour déterminer l'effet du diamètre de l'orifice sur la courbe d'étalonnage sans dimensions et sur les réglages des échantillonneurs D-77, DH-81 et autres, utilisés par les organismes de collecte de données.

TABLE OF CONTENTS

1.0 INTRODUCTION

Suspended solids play a strong role in the biological and chemical balance of the aquatic environment. The important components of the suspended load for geochemical transport are silts, clays and particulate organic carbon (Droppo and Ongley 1989 and Ongley *et al.* 1981). These components are also identified as important for the transport of contaminants such as heavy metals, phosphorous and a wide range of synthetic, organic substances, especially where sediment transport is high (Frostrer and Wittman 1981, Frank 1981, Kuntz and Wary 1983, Allen 1986, Ongley *et al.* 1988, Krishnappan and Ongley 1988). In fine sediment transport the source of fine sediment fractions is mainly from off-channel sources, such as soil erosion. The transport capacity of river flows virtually always exceeds the supply rate of these sources (Krishnappan and Ongley 1988) and the effects on water quality extend for long distances down stream.

Accurate measurement of suspended solids concentration and distribution is critical in the study of sediment and contaminant transport. A variety of samplers for measuring suspended sediment concentration in rivers have been developed over the last fifty years (U.S.A.C.E. 1941, T.C.P.S.M. 1969, Guy and Norman 1970 and Cashman 1988). However, only two depth integrating type samplers classified by the U.S. Federal Inter-Agency Sedimentation Project as US D-77 and US DH-81 are relevant to the sampling of contaminated sediments because all components exposed to the water sample are of autoclavable plastics. The D-77 sampler was designed to collect large volume samples from streams at near freezing temperatures but can be used under low flow conditions at higher temperatures. The DH-81 sampler is an adaptation of the D-77 and is used for sampling normal flow in small to intermediate sized streams or through the ice, suspended with a wading rod. The D-77 sampler has been found to over-sample the flow rate at low velocities and under-sample the flow rate at higher velocities and this discrepancy is known to be water temperature dependent (Skinner 1979). A similar behaviour has been observed by the writers with the DH-81 sampler. These departures from iso-kinetic sampling are a source of concern, particularly as far as the fine grained sediments are concerned. These fine sediments are frequently flocculated (Droppo and Ongley 1989). Flocculation changes the effective grain size of the particles and consequently their settling velocities. As a result, over-sampling at

low velocities may actually mis-represent the true sediment size and structure in the water column. Over or under-sampling may also mis-represent any short term temporal variations in sediment and water chemistry which may exist during the vertical transit time of the sampler. This size and/or chemical mis-representation can have significant implications from a water and sediment quality perspective. Therefore, it is important that a sampler be iso-kinetic at all velocity ranges.

Sediment loads and properties as well as water chemistry of small rivers in Ontario are an important component of the research program at the National Water Research Institute in which the DH-81 suspended sediment sampler is used extensively. In an effort to improve the performance of this type of sampler, preliminary tests were conducted in the towing tank of the Institute's hydraulics laboratory to investigate the possibility of obtaining iso-kinetic calibrations. The results of this study are presented in this report.

2.0 PRELIMINARY CONSIDERATIONS

The purpose of the suspended sediment sampler is to obtain a sample that is representative of the water-sediment mixture moving in the vicinity of the sampler. During the sampling, a volume of the water-sediment mixture is collected in the sampler over a measured interval of time, using the equal transit rate (ETR) sampling method (Guy and Norman 1970). From the measured volume and time the flow rate into the sampler is then determined. The velocity of the flow through the nozzle is computed by dividing the flow rate by the cross-sectional area of the nozzle hole. The sediment flux is the product of the sediment concentration of the collected sample and the nozzle velocity.

Suspended sediment samplers are operated on the premise that the velocity of flow through the nozzle is equal to the velocity of the stream flow surrounding the nozzle. This condition is known as iso-kinetic sampling. For sediment sampling quality control, nozzle velocity, V_n, and the stream flow velocity, V_s, are expressed as a ratio given by

$$K = \frac{V_n}{V_s} \tag{1}$$

where K is the sampler performance coefficient. For iso-kinetic conditions, $K = 1$ and it is assumed that the flow entering through the nozzle contains the same sediment-water mixture as the stream flow being sampled. When $K > 1$ the sampler will under-sample the suspended sediment concentration, whereas when $K < 1$ the sampler will over-sample as shown in Figure 1 (Beverage and Futrell 1986). The error in sampling sediment concentration is shown to vary with particle size. When particles are in the silt and clay sizes (ie: particle diameter less than 0.063 mm) the error in sampling is within 5 percent if the performance coefficient is in the range $0.4 < K < 4.0$. The curves also show that errors in sample concentration becomes increasingly sensitive to the value of K as the particle size increases. For a grain size of 0.45 mm, values of the sampler performance coefficient should be in the range $0.88 < K < 1.20$ in order to maintain a sediment concentration sampling accuracy of 5 percent.

The curves in Figure 1 are based on particles having a constant density and therefore do not truly reflect conditions pertaining to the silt and clay sizes. Fine sediments are frequently flocculated (Droppo and Ongley 1989). Particles are

bonded together to produce single units called flocs. These flocs behave as single particles having an effective diameter many times larger than the original, component particles but having a lower density depending on their compactness. The tendency toward larger sampling errors as a result of increased particle size is offset by the lower density of the flocs. However, for the silt and clay sizes, sampling errors greater than those indicated in Figure 1, can be expected.

The reasons for these effects at different values of K are as follows: If $K = 1$, the stream flow will pass straight into the nozzle while any stream lines on either side of the nozzle intake will be deflected as shown in Figure 2(a). For this condition the trajectories of the sediment particles are parallel to the stream lines of the flow entering the nozzle. As a result the sampler collects the correct proportion of water and sediment particles. When $K < 1$, the velocity in the nozzle will be slower than the stream flow velocity and, as a result, an area of stagnation will develop at the head of the nozzle as shown in Figure 2(b). In this case the stream lines of the approaching flow will be deflected ahead of the nozzle entrance. However, the sediment particles, because of their inertia, will tend to continue on their original path toward the nozzle entrance. As a result, for a given sampling time, the sampler will under-sample the water volume but collect a larger proportion of sediment particles, resulting in over-sampling of the sediment concentration. Finally, when $K > 1$, the velocity in the nozzle will be greater than that of the approaching flow and stream lines in the vicinity of the nozzle will converge toward the nozzle intake as shown in Figure 2(c). Once again the sediment particles will resist the sudden change in direction and the increase in water flow through the nozzle will not be accompanied by a corresponding increase in sediment particles. As a result, the sampler will under sample the sediment concentration.

In general, particle sizes in suspension are largely a function of flow velocity and level of turbulence, and therefore, a wide range of particle sizes can be obtained in a given sample. It is important to ensure that the samplers are capable of sampling iso-kinetically.

3.0 EXPERIMENTAL EQUIPMENT AND PROCEDURE

3.1 Towing Tank

The towing tank used to test the sampler is 122 m long by 5 m wide and is constructed of reinforced concrete founded on piles. The full depth of the tank is 3 metres, of which 1.5 metres are below ground level. Normally the water depth is maintained at 2.7 metres. Concrete was chosen for its stability and to reduce possible vibrations and convection currents.

At one end of the tank is an overflow weir. Waves arising from towed objects and their suspensions are washed over the crest, thereby reducing wave reflections. Parallel to the sides of the tank perforated beaches serve to dampen lateral surface wave disturbances.

3.2 Towing Carriage

The carriage is 3 metres long, 5 metres wide, weighs 6 tonnes and travels on four precision machined steel wheels. The carriage is operated in three overlapping speed ranges:

0.005 m/s - 0.06 m/s
0.05 m/s - 0.60 m/s
0.50 m/s - 6.00 m/s

The maximum speed of 6.00 m/s can be maintained for 12 seconds. Tachometer generators connected to the drive shafts emit a voltage signal proportional to the speed of the carriage. A feedback control system uses these signals as input to maintain constant speed during tests.

The average speed data for the towing carriage is obtained by recording the voltage pulses emitted from a measuring wheel. This wheel is attached to the frame of the towing carriage and travels on one of the towing tank rails, emitting a pulse for each millimeter of travel. The pulses and measured time are collected and processed to produce an average towing speed with a micro computer data acquisition system. Analysis of the towing speed variability by Engel (1989), showed that for speeds between 0.2 m/s and 3.00 m/s, the error in the mean speed was less than 0.15 percent at the 99 percent confidence level. Occasionally, these tolerances are exceeded as a result of irregular occurrences such as "spikes" in the data transmission system of the towing carriage. Tests with such anomalies

are recognized by the computer and are automatically abandoned.

3.3 The DH-81 Sampler and Appurtenances

The sampler consists of a DH-81 adapter, a US D-77 cap, a standard 7.94 mm inside diameter nozzle, a plastic "mason-jar" threaded bottle with 3 litre capacity and a wading rod. The components of the sampler are given in Figure 3 and the assembled sampler is given in Figure 4.

The US DH-81 sampler is designed to sample low velocity rivers by wading or by sampling through the ice cover (Cashman 1988). The sampler allows for large sample volumes (2700 ml), providing the large samples required for sedimentological analysis. When used in conjunction with a plastic bottle the sampler is useful for chemical and biological studies as all the components which contact the water sample are composed of autoclavable plastic. When the sampler is lowered into the flow, air is expelled through a 3.0 mm diameter air vent at the top of the sampler cap. A small "horn" protruding from the sampler cap just ahead of the air vent presents a "bluff" body to the flow resulting in a small negative pressure pocket immediately behind it. This creates a "suction" effect which effectively reduces the energy drop through the air vent. Finally, the air vent outlet is located about 2 cm above the centre-line of the nozzle flow passage. This creates a small positive, net hydro-static pressure which is constant regardless of the depth of the sampler.

3.4 Effect of Flow Depth

The D-77 and the DH-81 sampler are open to the outside environment during the depth integrated sampling process. As a result, the air volume inside the samplers is subject to the effect of pressure changes as the sampler is lowered and raised through the flow. Initially, at the surface, the internal cavity of the sampler is at atmospheric pressure because the sampler is open to the air through the nozzle and the air vent. As the sampler is submerged and travels toward the stream bed, the pressure inside the sampler increases in proportion to the flow depth. The increase in static pressure compresses the volume of air in the sampler and this causes an inflow of water in excess of that expected due to the net head (H_s + velocity head; where H_s is the static head at the nozzle equal to the difference in elevation of the centre-line of the nozzle and the air vent) alone.

During the present tests this problem was eliminated by holding the test sampler fixed at the minimum possible depth of of 0.2 m.

3.5 Test Series No.1

For a given nozzle the volume of water that can enter the sampler bottle in a given period of time should depend, among other things, on the the physical properties of the nozzle and the air vent. In order to determine the effect of the vent size on the sampling rate, 5 sets of tests were conducted for a range of towing velocities (0.2 m/s, 0.4 m/s, 0.6 m/s, 0.8 m/s and 1.0 m/s) with a range of air vent diameters (1.0 mm, 1.5 mm, 2.0 mm, 2.5 mm and 3.0 mm). The nozzle diameter was kept fixed at 7.5 mm (5/16"). To vary the size of the vent hole, the existing exhaust port was drilled and tapped to receive a 6.4 mm (1/4") Allen key plug. Five such plugs were prepared, each with a hole drilled concentric with its longitudinal axis, to provide the new vent hole of the desired size. For each case the Allen key plug was screwed into place so that the bottom of the plug was flush with the invert of the original vent passage.

Each series of experiments for a given air vent diameter was considered a test. At the beginning of each test, the appropriate plug was inserted into the sampler cap and the sampler assembled in its standard configuration. Each test was begun at the nominal towing velocity of 0.2 m/s and continued at intervals of 0.2m/s to the maximum velocity of 1.0 m/s.

Once the sampler was prepared, the towing carriage was set into motion. Once the carriage had reached its pre-set velocity, the sampler was submerged and held at 0.2 m below the surface of the water for a set period of time. Care was taken that the bottle was never more than 2/3 full to ensure that there was no interference in the air flow through the vent due to over-filling. The tests were conducted in a towing tank because this afforded better control over the reference velocity than can be obtained in a flume. It has been shown that there is little difference between sampler calibrations obtained in a flume and in a towing tank (Beverage and Futrell 1986). Although, this procedure does not simulate actual stream sampling methods, it does, however, allow the operation of a sampler at a constant velocity. When the set period of sampling time had expired the sampler was removed from the water and the volume of water determined with a 1000 ml graduated cylinder. The velocity of flow through the sampler nozzle was then

computed from the equation

$$V_n = \frac{1.273 V_w}{d^2 t_s} \tag{2}$$

where d = the diameter of the flow passage through the nozzle in mm, V_w = the volume of water collected in c.c., t_s = the time over which the sampler was submerged in seconds. Each test was repeated once to ensure satisfactory repeatability of the testing procedure. The test data are given in Table 1.

Test Series No.2

The procedure in Test Series No.1 provided information on the effect of changing the air vent diameters. However, such information does not provide very useful data for direct calibration of sediment samplers. A more direct method is to vary the size of the air vent by means of a valve. The use of a valve is equivalent to having an infinite number of discrete air vent sizes as opposed to the limited number obtained by the method used in Test Series No.1. The valve was devised by using the 6.4 mm (1/4") Allen key plug with the 3.0 mm diameter hole from the previous test series. The control of the air flow was achieved by turning the plug with an Allen key, thus raising or lowering the plug in the tapped hole and decreasing or increasing the blockage of the internal air tunnel. The valve was considered fully closed when the plug was turned until the internal air tunnel was completely obstructed. Alternately, the valve was considered to be fully open when the bottom of the plug was in the same position as that used in Test Series No. 1. The position of the Allen key was carefully noted in terms of degrees of rotation. When the valve was closed the angle of rotation, Θ, of the valve was taken to be zero degrees. When the valve was fully open, the total rotation of the valve stem (Allen key) was 3.67 turns or 1320 degrees. The valve settings were expressed as a fraction of the fully open setting, expressed as Θ_r. The sampler cap and the provisional valve, extending into the internal air tunnel, are shown in Figure 5.

To calibrate the sampler valve it was necessary to find the valve setting at a particular velocity for which the nozzle velocity was equal to the towing velocity (ie: $K = 1$). This required a trial and error procedure until the desired valve setting was obtained. Once this was accomplished, a total of five samples were collected at the same velocity and the nozzle velocity computed each time. The procedure was used with towing velocities of 0.3 m/s, 0.4 m/s, 0.6 m/s 0.8 m/s

and 1.0 m/s. The nozzle velocities were determined in the same way as in Test Series No.1. The data are given in Table 2.

4.0 DATA ANALYSIS

4.1 Nozzle Velocity Versus Carriage Velocity

Examination of the data in Table 1 reveals that the performance tests in the towing tank can be conducted with a high degree of repeatability thus confirming that this method is suitable for sediment sampler calibration. The data in Table 1 were plotted as V_n vs. V_s (where now V_s = towing carriage velocity) with the vent hole diameter as a parameter in Figures 6. On this plot, the data are given together with the +/- 15 percent error boundary for the nozzle velocity and the straight line signifying perfect agreement between the nozzle velocity and carriage velocity (ie: $K = 1$). The data clearly show the effect of the air vent diameter on the performance of the sediment sampler. The nozzle velocity increases as the carriage velocity increases with the rate of change gradually increasing as the air vent diameter increases. At a given carriage velocity, the nozzle velocity increases as the air vent diameter increases with the rate of change decreasing as the vent diameter increases.

For the smallest diameter of 1.0 mm tested, the nozzle velocity and carriage velocity are virtually identical when the latter is 0.2 m/s. As the carriage velocity increases above 0.2 m/s, the agreement between the two velocities progressively deteriorates, with the nozzle velocity always being smaller than the towing velocity. When the air vent diameter is 1.5 mm close agreement between the nozzle and carriage velocity is obtained when the latter is 0.4 m/s. For carriage velocities less than about 0.4 m/s, nozzle velocities are above the line of perfect agreement, whereas for carriage velocities greater than 0.4 m/s, nozzle velocities are below the 1:1 line with the deficit increasing as the carriage velocity increases. When the vent diameter is increased to 2.0 mm, perfect agreement is obtained at about 0.55 m/s. For carriage velocities less than 0.55 m/s, nozzle velocities are higher with the excess increasing as the carriage velocity decreases. When the carriage velocity is greater than 0.55 m/s, the nozzle velocities are always below the 1:1 line with the deficit increasing gradually. When the vent diameter is 2.5 mm, perfect agreement is obtained when the carriage velocity is 0.8 m/s. For velocities less than this, nozzle velocities are above the 1:1 line with the excess again increasing as carriage velocity decreases. For carriage velocities greater than 0.8 m/s, nozzle velocities are always smaller than the reference velocity. Finally, when the vent

diameter is 3.0 mm, perfect agreement is obtained when the carriage velocity is 1.0 m/s. For carriage velocities less than this, nozzle velocities are always above the line of perfect agreement with the excess increasing as the reference velocity decreases. For carriage velocities greater than 1.0 m/s, as observed for the previous vent diameters, the opposite is true.

The behaviour of the DH-81 sampler is similar to that of the D-77. Both samplers have similar nose-cap features, use a 7.94 mm (5/16") nozzle and have a fixed air vent diameter of 3.0 mm. A typical calibration of a D-77 sampler developed by Skinner (1979) is given in Figure 7 for a water temperature of about 1° C. Super imposed on Figure 7 are the data obtained from Figure 6 for the case of the 3.0 mm diameter air vent obtained at a water temperature of about 21° C. Both samplers exhibit the same trend with the DH-81 sampler having slightly larger nozzle velocities. This is thought to be due to the difference in water temperatures.

4.2 Condition for Iso-Kinetic Sampling

The required conditions for perfect agreement with respect to the data in Figure 6 are fully specified by a plot of the corresponding air vent diameter as a function of the carriage velocity. Such a plot is given in Figure 8 for the five different vent hole diameters investigated. The plotted points were connected by a smooth curve showing that the relationship between the vent diameter and the carriage velocity is linear. The curve shows that for a given flow velocity a vent hole of a particular diameter is required in order to achieve iso-kinetic conditions. It is also clear from Figure 8 that in the region above the linear curve one obtains conditions for $K > 1$, whereas conditions in accordance with $K < 1$ are obtained below the curve.

Clearly, it is not possible to have an air vent of a particular diameter for all flow velocities. At best, one could consider each vent diameter to be applicable over a certain range of flow velocity with the extent of each velocity range depending on the sampling accuracy required. In Figure 6 it can be seen that when the vent diameter is 2.0 mm, nozzle velocities are within 15 percent of the carriage velocity for values of 0.4 m/s to 1.0 m/s. This translates into values of K in the range $0.85 < K < 1.15$. Examination of Figure 1 suggests that this may provide sufficient accuracy in the sampled sediment concentration for velocities of

0.4 m/s to 1.0 m/s. When the carriage velocity is 0.2 m/s, the nozzle velocity obtained is about 0.41 m/s, representing an error of 105 percent, which translates into $K = 2.05$. According to Figure 1, such a value of K is acceptable for clay to silt size particles, however, as flow velocities approach values between 0.2 m/s to 0.4 m/s, particle sizes can be expected to be larger and values of K in the range $0.85 < K < 1.15$ would be more desirable. Further examination of Figure 6 reveals that selection of another air vent diameter would not be practical, because at carriage velocities less than 0.4 m/s, for each chosen value of air vent diameter, nozzle velocities would be within 15 percent error envelopes over a very narrow range of the reference velocities. Some improvement can be achieved by using an air vent diameter of about 1.50 mm at flow velocities of 0.4 m/s and less. This would ensure that the nozzle velocities would be inside the 15 percent error bands for flow velocities between 0.3 m/s and 0.4 m/s and reduces the value of K from 2.05 when the vent diameter is 2.0 mm to 1.63 when the vent diameter is 1.5 mm. At the very low flows, there is also a concern about flocculation, resulting in effective particle diameters larger than the individual component particles. These larger particles further increase the need for iso-kinetic sampling for flows near velocities of 0.2 m/s. The data in Figure 6 suggest that in this case an air vent diameter of 1.0 mm should be used. Although, using different air vent diameters provides some improvement, it is obvious that the use of discrete air vent sizes is not a fully satisfactory solution.

4.3 Continuous Air Vent Control

The data in Table 2 were organized so that the rotation of the air valve at any given position was expressed as a fraction of the fully open position. The data were then plotted as Θ_r versus the carriage velocity in Figure 9. A smooth curve was fitted through the plotted points to facilitate the analysis. The curve represents the flow control curve for the DH-81 sampler, showing a gradual increase in Θ_r as the carriage velocity increases, with the rate of change in Θ_r increasing or, conversely, the sensitivity of the valve decreasing. When the carriage velocity is 1.0 m/s, the curve indicates that the upper limit of the air valve has been virtually reached. During the tests it was not possible to obtain consistent results at a carriage velocity of 0.2 m/s. However, tests at a velocity of 0.3 m/s were successful. Therefore, for the present valve configuration it was concluded that

the lowest operating limit is about 0.25 m/s. It is most probable, that at such low velocities, the total pressure head driving the flow into the sampler nozzle is not great enough to overcome the energy losses of the air flow passing through the valve. Further development work is required to overcome this problem at low flow velocities.

Although the air valve has been crudely contrived, the data in Figure 9 indicate that a consistent relationship between the valve opening and the flow velocity is possible. Therefore, such a valve is a viable and practical alternative to the discrete air vent sizes discussed in the previous section.

The mean nozzle velocities obtained at each valve setting for a particular carriage velocity are plotted as Figure 10. Tests at each carriage velocity were conducted five times. All points fall on the line of perfect agreement, signifying a value of $K = 1$. These results further substantiate that the DH-81 sediment sampler performance can be controlled with a high degree of repeatability by using an air vent valve. Clearly, for this type of sampler, the control of the flow into the sampler is governed by the valve and not by the hydraulic characteristics of the nozzle.

A curve of Θ_r vs. V_s, as given in Figure 9, represents the calibration curve for a particular sampler. Further tests should be conducted to see if a single generic curve can be used for all DH-81 samplers.

5.0 GENERAL CALIBRATION EQUATION

5.1 Dimensional Analysis

When the sampler is submerged with the nozzle pointed directly into the flow, the water sediment- mixture enters the sampler as air is exhausted under the combined effect of a) the dynamic positive head of the flow at the nozzle entrance, b) hydro static pressure head because of the difference in elevation between the nozzle intake and the air vent and c) a negative pressure head at the air outlet port immediately behind the "horn" intended for this purpose. The various important features of the DH-81 sampler are given in Figure 11. The total pressure head is reduced by the hydraulic losses due to flow contraction, expansion and frictional losses at the nozzle as well as contraction and expansion losses at the air vent passage. In some samplers, changes in energy losses of the nozzle can be effected by changing the nozzle intake diameter and changing its entrance and outlet geometry (Beveridge and Futrell 1986, Engel and Zrymiac 1989, Engel 1990). It has already been shown that, for the 7.5 mm (5/16") nozzle used with the DH-81 sampler, substantial changes in the energy losses at the air vent can be effected by changing the diameter of the air vent.

In general, the nozzle velocity for the DH-81 sampler can be expected to depend on the set of variables expressed in the following functional relationship:

$$V_n = f\left(V_s, d, h, D, b, \phi, \sqrt{U^2}, \rho_a, \mu_a, \rho_w, \mu_w\right) \tag{3}$$

where f denotes a function, d = the diameter of the nozzle flow passage, h = the depth of water above the air vent, b = the length of the nozzle, ϕ = the angle of the longitudinal axis of the nozzle with the horizontal, $\sqrt{U^2}$ = the turbulence of the stream flow as the root mean square of the velocity fluctuations in the streamwise direction, D = the diameter of the air vent, ρ_a = the density of the air inside the sampler bottle, μ_a = the dynamic viscosity of the air in the sampler bottle, ρ_w = the density of the water and μ_w = the dynamic viscosity of the water. The geometric parameters of equation (3) are shown in Figure 11. Using dimensional analysis, one obtains the dimensionless relationship:

$$\frac{V_n}{V_s} = f_1\left(\frac{h}{d}, \frac{b}{d}, \phi, \frac{\sqrt{U^2}}{V_s}, \frac{D}{d}, \frac{V_s d \rho_w}{\mu_w}, \frac{V_s d \rho_a}{\mu_a}, \frac{\rho_a}{\rho_w}, \right) \tag{4}$$

where f_1 denotes a dimensionless function for a particular sampler. Beverage and Futrell (1986) have shown that results from tests in towing tanks are not significantly different from results of tests conducted in turbulent flows in flumes. Therefore, the variable $\frac{\sqrt{U^2}}{V_s}$ in equation (4) is not very important and can be omitted from further considerations. The depth of submergence of the sampler was kept at 0.2 m and therefore the effect of $\frac{h}{d}$ will be negligible and may also be eliminated from equation (4). Examination of data by Engel and Zrymiac (1989) and Engel (1990) indicate that the discharge coefficient of nozzles is only mildly dependent on the Reynolds number $\frac{V_s d \rho_w}{\mu_w}$ and over the range of operating temperatures the ratio $\frac{\rho_a}{\rho_w}$ does not vary significantly. As a result, these last two variables may also be omitted from equation (4). Combining equations (3) and (4) one obtains

$$K = f_2\left(\frac{b}{d}, \phi, \frac{D}{d}, \frac{V_s d \rho_a}{\mu_a}\right) \tag{5}$$

where f_2 denotes another dimensionless function. In general, equation (5) shows the various dimensionless variables that can affect the value of K. In this study, tests were conducted with a sampler having fixed values of $\frac{b}{d}$ and $\phi = 0$. Therefore for present purposes equation (5) can be reduced to

$$K = f_3\left(\frac{V_s d \rho_a}{\mu_a}, \frac{D}{d}\right) \tag{6}$$

where f_3 denotes another dimensionless function. For the case of valve control the effective vent opening is governed by the adjustment of the air vent valve. Therefore, by introducing the dimensionless valve setting Θ_r, equation (6) may now be expressed in an alternate form as

$$K = f_4\left(\frac{V_s d \rho_a}{\mu_a}, \Theta_r\right) \tag{7}$$

where f_4 denotes another dimensionless function. Finally, the calibration curve must exist for the special case of $K = 1$ and for this case, one may now write the dimensionless calibration curve as

$$\Theta_r = f_5\left(\frac{V_s d \rho_a}{\mu_a}\right) \tag{8}$$

where f_5 denotes another dimensionless function.

Equation (8) states that the calibration of the DH-81 sampler should depend on a single dimensionless variable based on the flow velocity, the nozzle diameter and the physical properties of the air in the sampler bottle. Such a relationship can be of considerable practical value because it accounts for the effects of water temperature which governs the air temperature, assuming that equilibrium between these two temperatures has been established at the beginning of sampling.

5.2 Relative Importance of Air Vent and Intake Nozzle

The data in Table 1 were used to compute the dimensionless variables given in equation (6). These values are given in Table 3. The data in Table 3 were plotted as K vs $\frac{V_o d \rho_a}{\mu_a}$ with $\frac{D}{d}$ as a parameter in Figure 12. Smooth curves were drawn through the plotted points resulting in a family of five curves. The curves clearly show, that values of K increase as values of $\frac{D}{d}$ increase for all values of $\frac{V_o d \rho_a}{\mu_a}$ with the rate of increase in K dimininshing as $\frac{D}{d}$ becomes larger. The dependence of K on $\frac{D}{d}$ shows that the inflow control is governed by the air vent and is independent of the nozzle. The decrease in dependence of K on $\frac{D}{d}$ suggests that there is a limiting value of $\frac{D}{d}$ after which the control at the air vent will shift to the intake nozzle. For the present tests, the diameter of the nozzle was 7.94 mm (5/16") and the maximum air vent diameter was 3.0 mm, resulting in the maximum value of $\frac{D}{d}$=0.378. The test results imply that the effect of the air vent may become negligible for diameters not much greater than 3.0 mm. Indeed, it is possible, that a limiting value of $\frac{D}{d}$ for air vent control may be of the order of 0.5, which represents a vent diameter of about 4 mm for the DH-81 sampler. The data further suggest that for a given air vent diameter, control can be shifted from air vent control to nozzle control by reducing the diameter of the intake nozzle. Indeed, many samplers presently in use by data gathering agencies, use three sizes of nozzles ((3.2 mm (1/8"), 4.8 mm (3/16"), 6.4 mm(1/4")) with a fixed air vent size. Such samplers are calibrated in towing tanks or flumes by adjusting both the air vent diameter and the hydraulic characteristics of the nozzles, in order to obtain performance as close to iso-kinetic as possible.

The curves in Figure 12 also show, that for a given value of $\frac{D}{d}$, K varies significantly with $\frac{V_o d \rho_a}{\mu_a}$. Over the range of test results, values of K decrease as $\frac{V_o d \rho_a}{\mu_a}$ increase with the rate of change decreasing as $\frac{V_o d \rho_a}{\mu_a}$ increases. The curves suggest that for each value of $\frac{D}{d}$, there is a critical value of $\frac{V_o d \rho_a}{\mu_a}$ at which K

becomes independent of $\frac{V_s d \rho_a}{\mu_a}$. When $\frac{D}{d} = 0.176$, the critical value of $\frac{V_s d \rho_a}{\mu_a}$ is about 600. The critical value of $\frac{V_s d \rho_a}{\mu_a}$ increases slightly as $\frac{D}{d}$ increases.

5.3 Dimensionless Calibration Curve

The data in Table 2 were used to compute the dimensionless variables given in equations (8). These values are given in Table 4. The data in Table 4 were plotted in Figure 13 as Θ_r vs. $\frac{V_s d \rho_a}{\mu_a}$. The form of the curve is similar to that of Figure 8. Values of Θ_r increase almost linearly as $\frac{V_s d \rho_a}{\mu_a}$ increases. When the latter reaches a value of about 500, Θ_r begins to increase sharply with further increases in $\frac{V_s d \rho_a}{\mu_a}$, indicating that there is a limiting value at which $\frac{V_s d \rho_a}{\mu_a}$ becomes independent of Θ_r. At this critical point, control of the flow into the sampler would change from the air vent to the intake nozzle.

The curve in Figure 13 has the advantage of including the fluid properties as well as the size of the nozzle. The curve indicates that for a given flow velocity, if the intake diameter of the nozzle is reduced, then $\frac{V_s d \rho_a}{\mu_a}$ is reduced and Θ_r must be reduced in accordance with the established calibration. In other words, a reduction in the size of the nozzle means a reduction in the rate of change of water volume inside the sampler and the valve opening must be reduced in accordance with the lower flow rate of escaping air, thereby ensuring that iso-kinetic conditions are maintained. It is also clear from the dimensionless calibration curve that water temperature must be considered when the sampler is used to allow for changes in fluid viscosity.

The dimensionless calibration curve in Figure 13 accounts for the fluid temperature. This can be demonstrated, with available data, by plotting the relationship given by equation (7) using the test data of the DH-81 sampler for the special case of the 3.0 mm diameter air vent. The appropriate data are plotted in Figure 14 as K vs. $\frac{V_s d \rho_a}{\mu_a}$. The data were obtained in water at a temperature of $20°C$. Superimposed on the plot are the data obtained from Skinner (1979) obtained with a D-77 sampler having the same diameter nozzle and sampler cap geometry at a water temperature of about $1°C$. The plot shows that K declines as $\frac{V_s d \rho_a}{\mu_a}$ increases with the rate of decrease diminishing. It is also quite evident that both sets of data collapse to form a single curve. This strongly suggests that a single dimensionless curve such as given in Figure 13 and 14 can be used to account for the changes in average air properties for all water temperatures likely to be

encountered during field operations. Separate curves for each temperature are no longer necessary. However, the general validity of the dimensionless calibration curve needs to be confirmed with additional tests. Tests should be conducted at several different water temperatures with at least three different nozzle sizes but having the same external geometry.

6.0 CONCLUSIONS

Tests, conducted in a towing tank, to establish a calibration curve for the US DH-81 suspended sediment sampler have led to the following conclusions:

6.1 The velocity of the flow passing through a sampler nozzle of a given size and geometry is controlled by the ability of the air to discharge through the air vent. For a given towing velocity, the rate of discharge could be controlled by changing the diameter of the air vent. The value of the sampling coefficient K increased as the diameter of the air vent was increased. The rate of change in K with change in air vent diameter was dependent on the towing velocity.

6.2 For a given air vent diameter the sampling coefficient K increased as the towing velocity increased. The rate of increase in K with the towing velocity increased slightly as the diameter of the air vent was increased.

6.3 For each of the air vent diameters used there was one towing velocity at which the sampler behaved iso-kinetically. At all other velocities values of K were greater or smaller than the ideal value of 1.0. Over the range of towing velocities from 0.2 m/s to 1.0 m/s, values of K varied from about 2.2 at a velocity of 0.2 m/s and an air vent diameter of 3.0 mm to a value 0.43 at a velocity of 1.0 m/s and an air vent diameter of 1.0 mm. The currently operational DH-81 sampler has a fixed air vent diameter of 3.0 mm and the values of K for velocities from 0.2 m/s to 1.0 m/s vary from 2.2 to 0.94 respectively.

6.4 Analysis of the data indicates that iso-kinetic sampling can be achieved over the operational velocity range of the sampler by controlling the air flow through the air vent with a calibrated valve. The sampler can therefore be calibrated in a towing tank by determining the required valve setting to obtain a value of $K = 1$ at each selected towing velocity.

6.5 Examination of the test data and data from the literature obtained for temperatures of $20°C$ and $1°C$ indicate that for a given flow velocity, nozzle velocities increase as the temperature increases. Dimensional analysis has shown that a dimensionless curve of K vs. $\frac{V_s d \rho_a}{\mu_a}$ for a given value of $\frac{D}{d}$ (V_s = towing velocity or

flow velocity, d = the internal diameter of the nozzle, D = the diameter of the air vent, ρ_a = the density of the air in the sampler and μ_a = the viscosity of the air in the sampler) can be used to represent the sampler performance. Each sush curve specifies the value of K and therefore the sampler performance at all water temperatures.

6.6 The validity of the dimensionless curves of K vs. $\frac{V_s d \rho_a}{\mu_a}$ guarantees the validity of a single dimensionless calibration curve of the air vent valve given as Θ_r vs. $\frac{V_s d \rho_a}{\mu_a}$. Therefore, with suitable modifications, the DH-81 suspended sediment sampler as well as the D-77 sampler can be used to sample virtually iso-kinetically over their full operating range. Theoretically, the dimensionless calibration curve should also be valid for different sizes of nozzles as long as the valve controls the flow into the sampler. Work is required to develop a suitable valve for the air vent control.

6.7 The results indicate that a critical value of $\frac{D}{d}$ exists at which the control of flow into the sampler changes from the air vent to the intake nozzle. This suggests that samplers in use today, other than the D-77 and the DH-81, are controlled either by the air vent or the intake intake nozzles depending on the size of the $\frac{D}{d}$ ratio (D= diameter of the air vent, d= diameter of the intake nozzle). Additional work is required to clearly establish the flow control regime.

ACKNOWLEDGEMENT

The writers are grateful to Dr. B.G. Krishnappan and Dr. M.G. Skafel for their thorough review of the manuscript and their many constructive comments and discussions. Assistance during the tests was provided by Clarence Bil, David Blais, Barbara Near and Stephen To. The photographs in Figures 3 and 4 were taken by Doug Doede. The writers appreciate their dedication to this project.

REFERENCES

Allan, R.J. 1986. The role of particulate matter in the fate of contaminants in aquatic ecosystems. Inland Waters Directorate, Scientific Series No. 142, National Water Research Institute, Canada Centre for Inland Waters, Burlington, Ontario, Canada.

Beverage, J.P. and Futrell, J.C. 1986. Comparison of Flume and Towing Methods for Verifying the Calibration of a Suspended Sediment Sampler. Water Resources Investigation Report 86 - 4193, USGS.

Cashman, M.A. 1988. Sediment Survey Equipment Catalogue. Sediment Survey Section, Water Survey of Canada Division, Water Resources Branch.

Droppo, I.G. and Ongley, E.D. 1989. Flocculation of Suspended Solids in Southern Ontario Rivers. In: Sediment and the Environment. Editors, R.J. Hadley and E.D. Ongley, International Association of Hydrologic Sciences. Third Scientific Assembly, Baltimore, Maryland, May 10 - 19, IAHS pup. No. 184.

Engel, P. 1989. Preliminary Examination of the Variability in the Towing Carriage Speed. NWRI Contribution 89 - 89, National Water Research Institute, Canada Centre for Inland Waters, Burlington, Ontario, Canada.

Engel, P. and Zrymiac, P. 1989. Development of a Calibration Strategy for Suspended Sediment Samplers - Phase I. NWRI Contribution 89 - 121, National Water Research Institute, Canada Centre for Inland Waters, Burlington, Ontario.

Engel, P. 1990. A New Facility for the Testing of Suspended Sediment Sampler Nozzles. NWRI Contribution 90 - 116. National Water Research Institute, Canada Centre for Inland Waters, Burlington, Ontario, Canada.

Frank, R. 1981. Pesticides and PCB in the Grand and Saugeen River Basins. J. Great Lakes Res. 7: 440 - 454.

Forstner, U. and Wittman, G.T.W. 1981. Metal Pollution in the Aquatic Environment. Springer - Verlag, New York.

Guy, H.P. and Norman, V.W. 1970. Field Methods for Measurement of Fluvial Sediment. Techniques of Water Resources Investigations of the United States Geological Survey, United States Government Printing Office, Washington, D.D.

Kuntz, K.W. and Warry, N.D. 1983. Chlorinated Organic Contaminants in Water and Suspended Sediments of the Lower Niagara River. J. Great Lakes Res.

9: 241 - 248.

Krishnappan, B.G. and Ongley, E.D. 1988. River Sediments and Contaminant Transport - Changing Needs in Research. NWRI Contribution 88 - 95. National Water Research Institute, Canada Centre for Inland Waters, Burlington, Ontario, Canada.

Ongley, E.D., Bynoe, M.C. and Percival, J.B. 1981. Physical and Geochemical Characteristics of Suspended Solids, Wilton Creek, Ontario. Can. J. Earth Sci. 18 : 1365 - 1379.

Ongley, E.D., Birkholz, D.A., Carey, J.H. and Samoiloff, M.R. 1988. Is Water a Relevant Sampling Medium for Toxic Chemicals An Alternative Environmental Sensing Strategy. J. Environ. Quality. 17(3): 391 - 401.

Skinner, J. 1979. Operating Instructions D - 77 Suspended Sediment Sampler, Federal Inter - Agency sedimentation Project, St. Anthony Falls Hydraulics Laboratory, Minneapolis, Minnesota, USA.

T.C.P.S.M., 1969. Sediment Measurement Techniques: A. Fluvial Sediment. Task Committee on Preparation of Sedimentation Manual, Committee on Sedimentation of the Hydraulics Division, Journal of the Hydraulics Division, Proceedings of the American Society of Civil Engineers, Vo. 95, No. HY5, pp 1477-1543.

U.S. Army Corps of Engineers, 1941. Laboratory Investigation of Suspended Sediment Samplers, Report No.5, St. Paul U.S. District Sub- Office, Hydraulics Laboratory, University of Iowa, Iowa City, Iowa.

TABLE 1
Test Data for the DH-81 Sampler
with Different Air Vent Diameters

V_w [c.c.]	t_s [s]	V_n [m/s]	V_s [m/s]	D [mm]	d [mm]
370	40.2	0.186	0.201	1.0	7.94
420	36.0	0.336	0.400	1.0	7.94
585	40.6	0.328	0.600	1.0	7.94
750	40.4	0.325	0.803	1.0	7.94
870	40.0	0.439	1.004	1.0	7.94
420	40.5	0.209	0.201	1.0	7.94
465	40.2	0.234	0.400	1.0	7.94
620	40.3	0.311	0.600	1.0	7.94
780	40.5	0.389	0.810	1.0	7.94
870	40.3	0.436	1.004	1.0	7.94
630	40.4	0.315	0.201	1.5	7.94
795	40.7	0.394	0.401	1.5	7.94
940	40.5	0.469	0.601	1.5	7.94
1110	40.5	0.554	0.803	1.5	7.94
1375	40.8	0.681	1.006	1.5	7.94
670	40.5	0.334	0.200	1.5	7.94
740	40.3	0.371	0.401	1.5	7.94
975	40.4	0.488	0.601	1.5	7.94
1058	40.3	0.530	0.810	1.5	7.94
1380	40.5	0.688	1.005	1.5	7.94
818	40.5	0.408	0.200	2.0	7.94
925	40.5	0.461	0.400	2.0	7.94
1125	40.5	0.561	0.600	2.0	7.94
1460	40.5	0.728	0.811	2.0	7.94
1720	40.5	0.858	1.007	2.0	7.94
790	40.4	0.395	0.201	2.0	7.94
923	40.5	0.460	0.401	2.0	7.94
1175	40.3	0.586	0.600	2.0	7.94
1465	40.4	0.728	0.812	2.0	7.94
1740	40.5	0.868	1.006	2.0	7.94

TABLE 1 contn'd
Test Data for the DH-81 Sampler
with Different Air Vent Diameters

V_w [c.c.]	t_s [s]	V_n [m/s]	V_s [m/s]	D [mm]	d [mm]
673	30.3	0.448	0.202	2.5	7.94
800	30.3	0.490	0.401	2.5	7.94
985	30.4	0.654	0.600	2.5	7.94
1208	30.6	0.797	0.809	2.5	7.94
1463	30.6	0.965	1.007	2.5	7.94
650	30.4	0.432	0.201	2.5	7.94
808	30.7	0.531	0.403	2.5	7.94
1000	30.3	0.667	0.600	2.5	7.94
1218	30.3	0.812	0.809	2.5	7.94
1425	30.4	0.947	1.008	2.5	7.94
705	30.3	0.470	0.201	3.0	7.94
860	30.4	0.571	0.401	3.0	7.94
1083	30.3	0.722	0.601	3.0	7.94
1370	30.3	0.880	0.809	3.0	7.94
1550	30.3	1.030	1.007	3.0	7.94
700	30.3	0.467	0.201	3.0	7.94
853	30.3	0.568	0.401	3.0	7.94
1055	30.3	0.703	0.601	3.0	7.94
1315	30.7	0.865	0.812	3.0	7.94
1500	30.3	1.000	1.007	3.0	7.94

V_w = volume of water collected in the sampler, t_s = time during which volume of water was collected, V_n = velocity of flow through the sampler nozzle, V_s = velocity of stream flow or towing carriage, D = diameter of the air vent, d = diameter of the flow passage of the nozzle.

TABLE 2
Test Data for the DH-81 Sampler
for Iso - Kinetic Conditions

V_w [c.c]	t_s [s]	V_n [m/s]	V_s [m/s]	Θ [degr.]	Θ_r [0]
660	40.2	0.332	0.301	150	0.114
635	40.3	0.318	0.302	150	0.114
640	40.1	0.322	0.301	150	0.114
610	40.1	0.307	0.301	150	0.114
630	40.3	0.316	0.301	150	0.114
780	40.2	0.392	0.400	240	0.182
798	40.3	0.400	0.401	240	0.182
798	40.3	0.400	0.400	240	0.182
798	40.1	0.402	0.401	240	0.182
820	40.2	0.412	0.400	240	0.182
1210	40.3	0.607	0.600	330	0.250
1208	40.2	0.607	0.600	330	0.250
1193	40.2	0.599	0.601	330	0.250
1205	40.3	0.604	0.600	330	0.250
1215	40.2	0.611	0.600	330	0.250
1623	40.1	0.817	0.809	690	0.523
1620	40.0	0.818	0.805	690	0.523
1640	40.2	0.824	0.808	690	0.523
1590	40.0	0.803	0.803	690	0.523
1598	40.5	0.797	0.810	690	0.523
1500	30.1	1.010	1.003	1320	1.00
1975	40.0	0.997	1.005	1320	1.00
1508	30.1	1.010	1.007	1320	1.00
1500	30.2	1.000	1.008	1320	1.00
1489	30.2	0.995	1.009	1320	1.00

Θ = total number of rotations of the vent valve expressed as an angle, Θ_r = valve setting expressed as a ratio of fully open condition.

TABLE 3
Dimensionless Variables for Test Series No. 1

K [0]	$\frac{V_s d \rho_a}{\mu_a}$ [0]	D/d [0]
0.925	107.3	0.126
0.840	213.6	0.126
0.547	320.4	0.126
0.404	428.8	0.126
0.437	428.8	0.126
1.040	107.3	0.126
0.835	213.6	0.126
0.518	320.4	0.126
0.480	432.5	0.126
0.434	534.0	0.126
1.567	107.3	0.189
0.982	214.1	0.189
0.780	320.9	0.189
0.690	428.8	0.189
0.677	537.2	0.180
1.670	106.8	0.189
0.925	214.1	0.189
0.812	320.9	0.189
0.654	432.5	0.180
0.685	536.7	0.189
2.040	106.8	0.252
1.153	213.6	0.252
0.935	320.4	0.252
0.898	433.1	0.252
0.852	537.7	0.252
1.965	107.3	0.252
1.147	214.1	0.252
0.977	320.4	0.252
0.897	433.6	0.252
0.863	537.2	0.252

TABLE 3 contn'd
Dimensionless Variables for Test Series No.1

K [0]	$\frac{V_a d \rho_a}{\mu_a}$ [0]	D/d [0]
2.217	107.9	0.315
1.222	214.2	0.315
1.090	320.4	0.315
0.985	432.0	0.315
0.958	537.7	0.315
2.149	107.3	0.315
1.318	215.2	0.315
1.112	320.4	0.315
1.004	432.0	0.315
0.940	538.3	0.315
2.338	107.3	0.378
1.424	214.1	0.378
1.201	320.9	0.378
1.088	432.0	0.378
1.023	537.7	0.378
2.323	107.3	0.378
1.416	214.1	0.378
1.170	320.9	0.378
1.065	433.6	0.378
0.993	537.7	0.378

K = sampler performance coefficient as given in equation (1), ρ_a = the density of the air in the sampler, μ_a = the dynamic viscosity of the air in the sampler.

TABLE 4
Dimensionless Variables for Test Series No.2

Θ [$deg.$]	V_s [m/s]	V_n [m/s]	K [0]	Θ_r [0]	$\frac{V_s d \rho_a}{\mu_a}$ [0]
150	0.301	0.319	1.060	0.114	160
240	0.401	0.401	1.000	0.182	213
330	0.600	0.606	1.009	0.250	319
690	0.807	0.812	1.006	0.522	430
1320	1.006	1.002	0.996	1.000	535

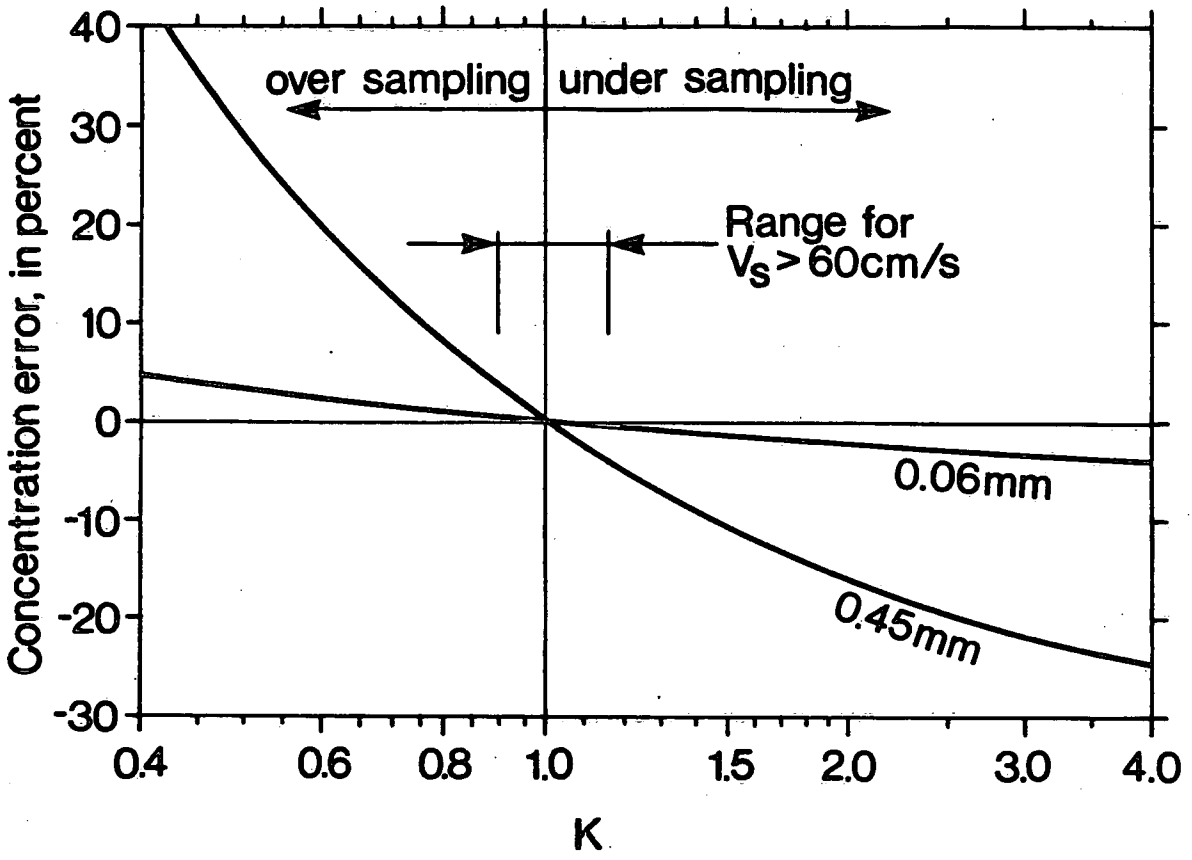

Figure 1 Effect of K and grain size on sampling error. (Beveridge and Futrell, 1986)

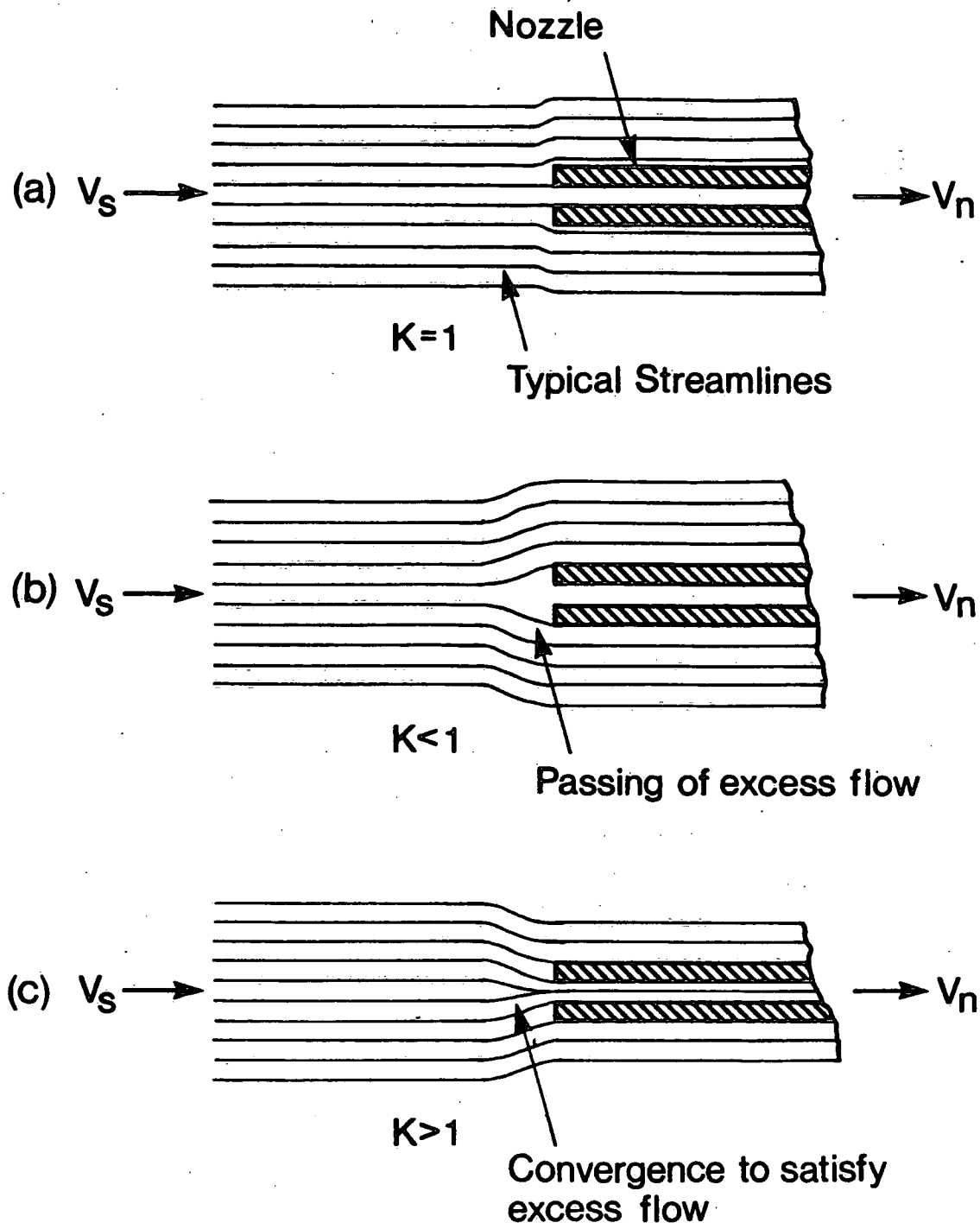

Figure 2 Flow pattern at nozzle nose for different values of K.

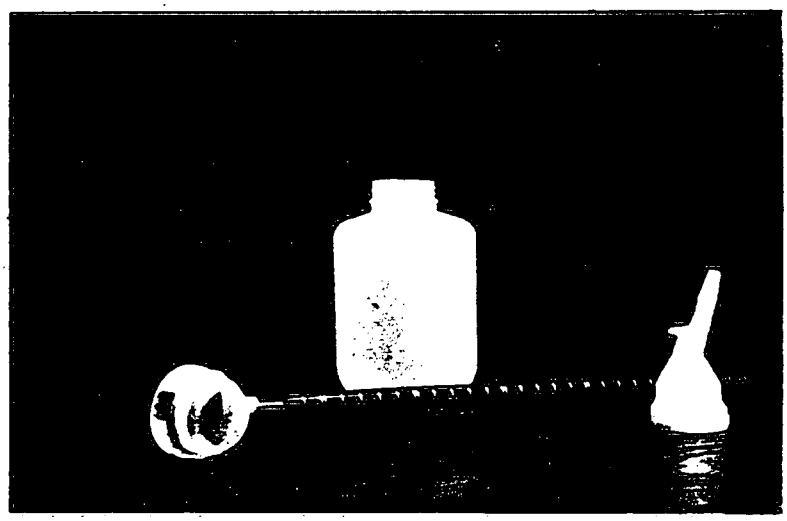

Figure 3 Components of USDH-81 sampler

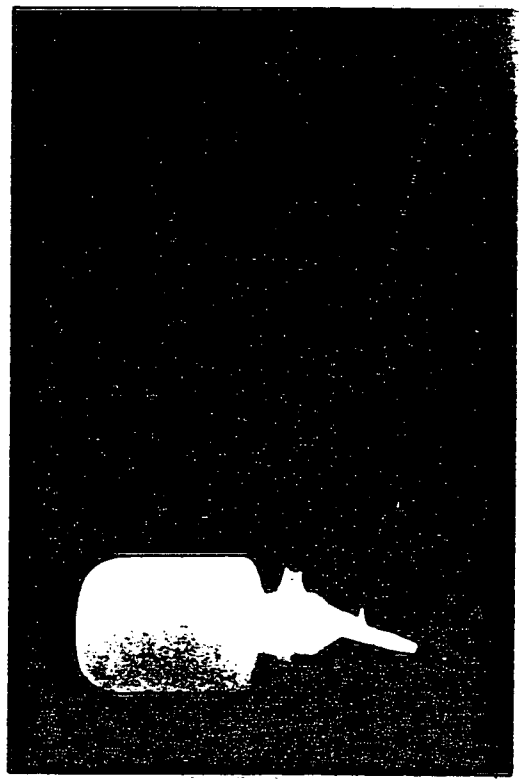

Figure 4 USDH-81 sampler assembled

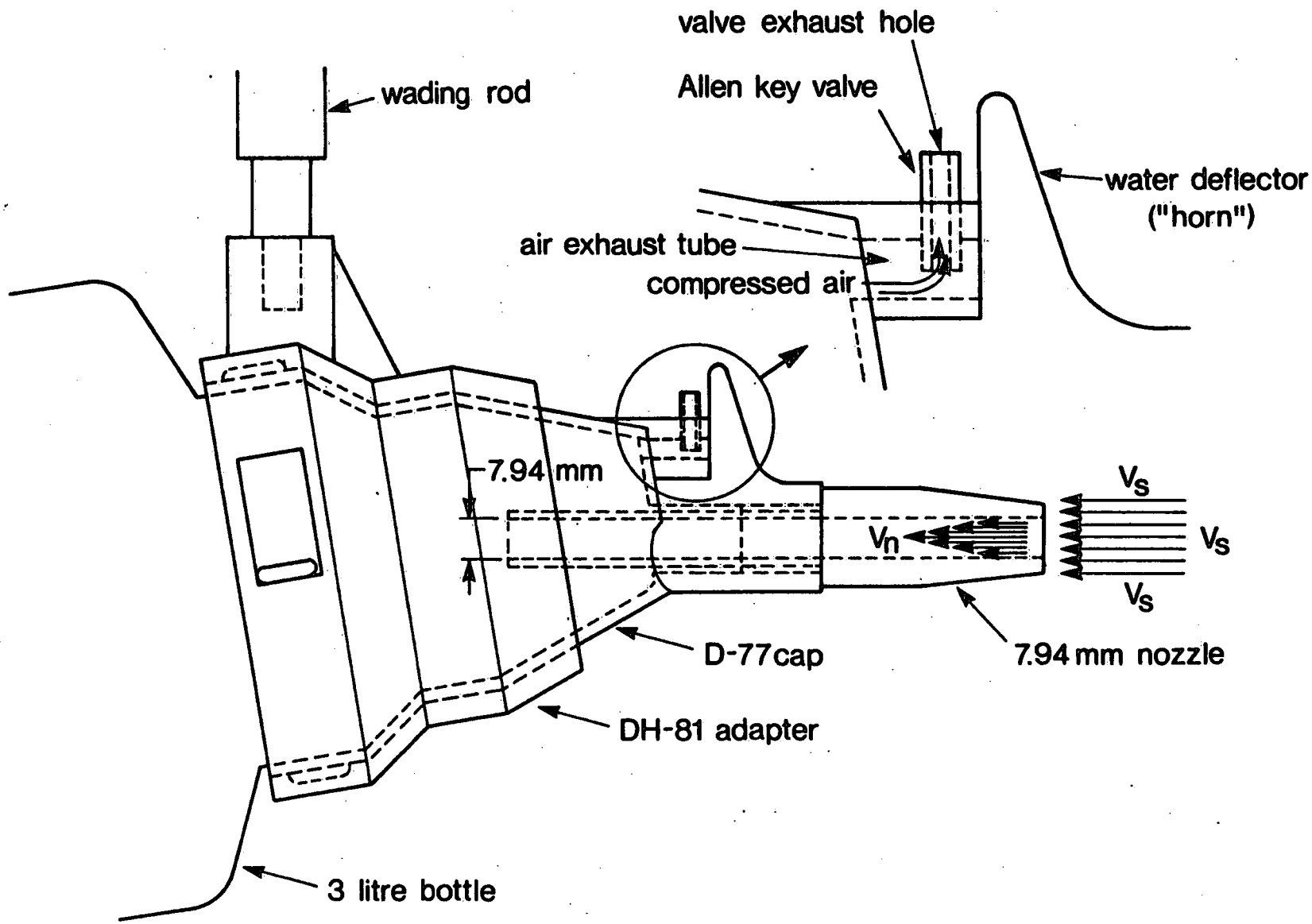

Figure 5 Air vent valve for DH-81 sampler tests

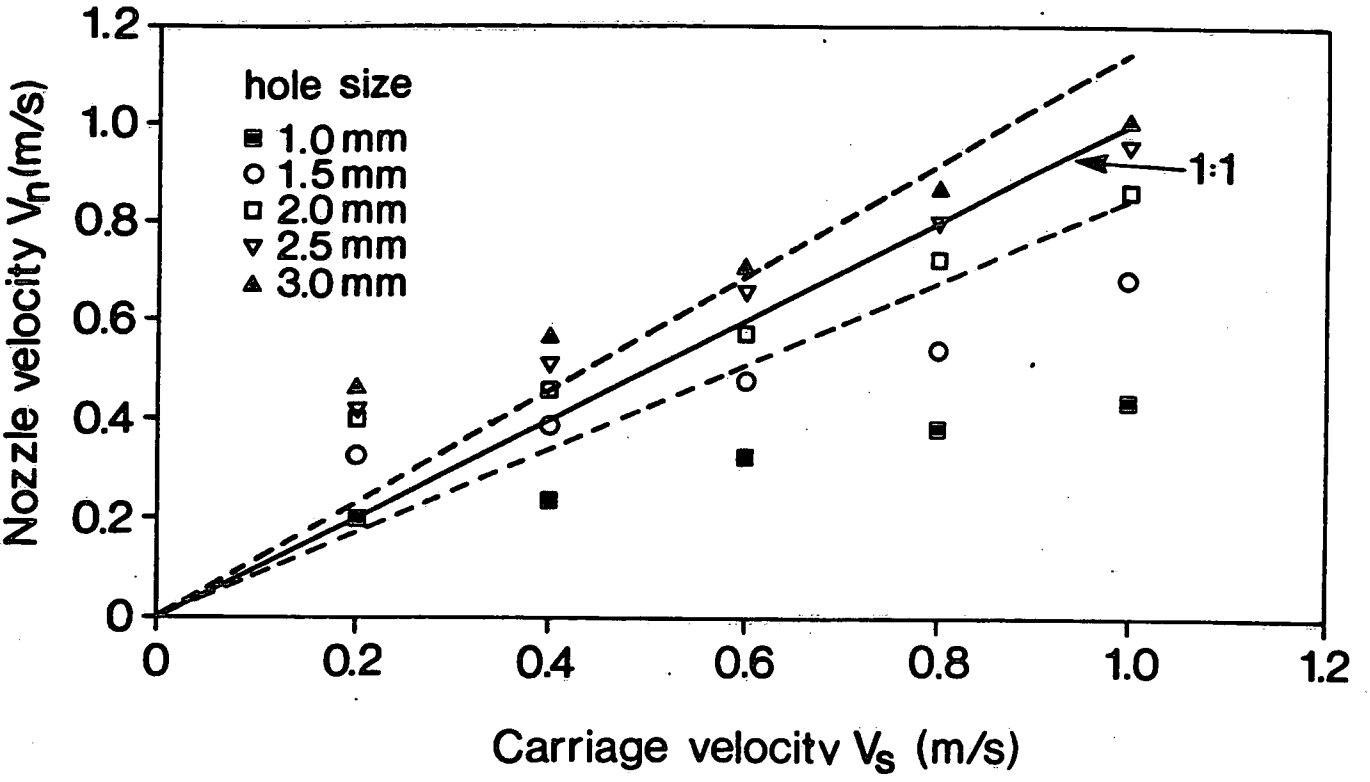

Figure 6 Nozzle velocity as a function of towing carriage velocity for different values of air vent diameter.

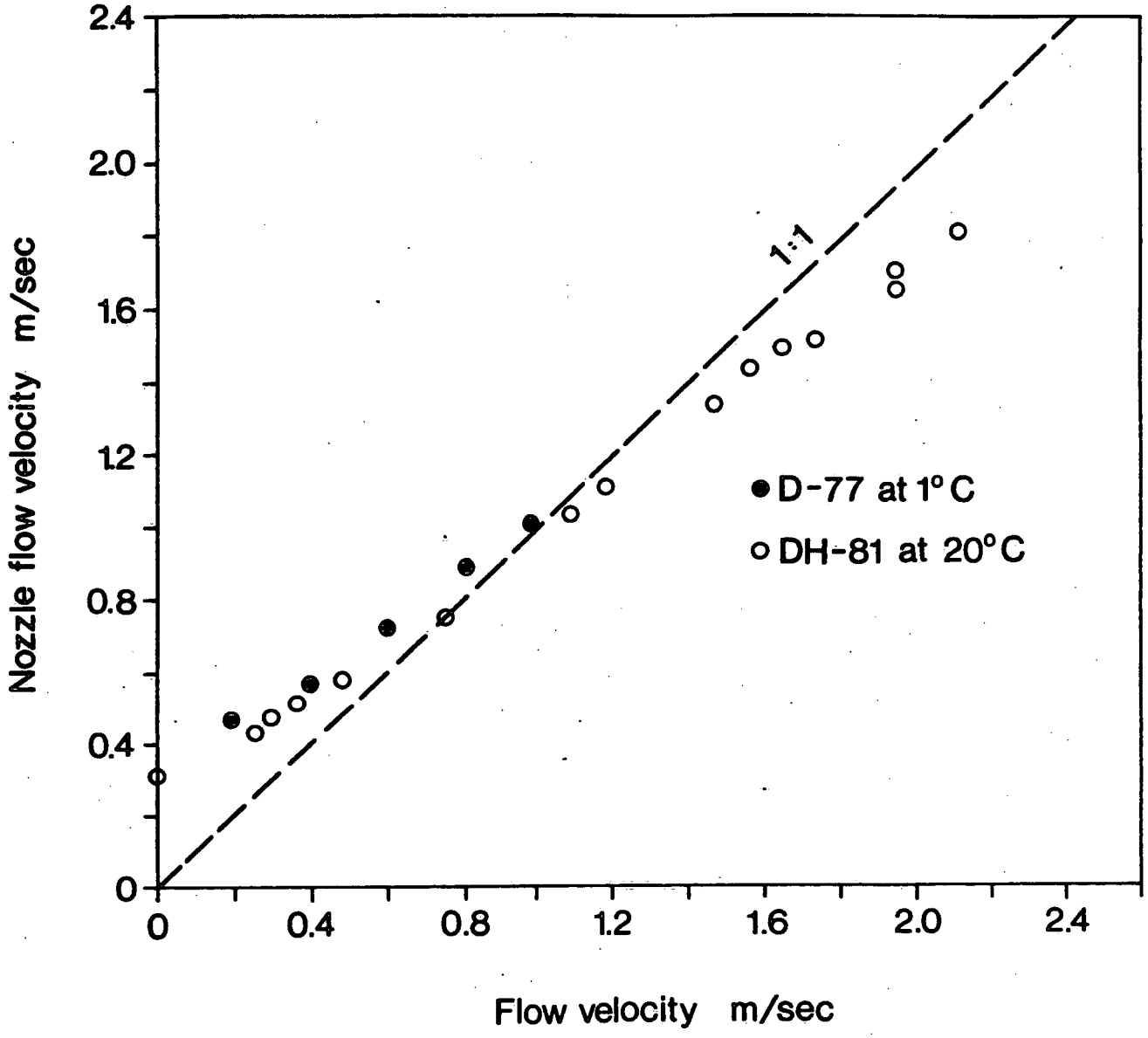

Figure 7 Behavior of US DH-81 and US D-77 samplers

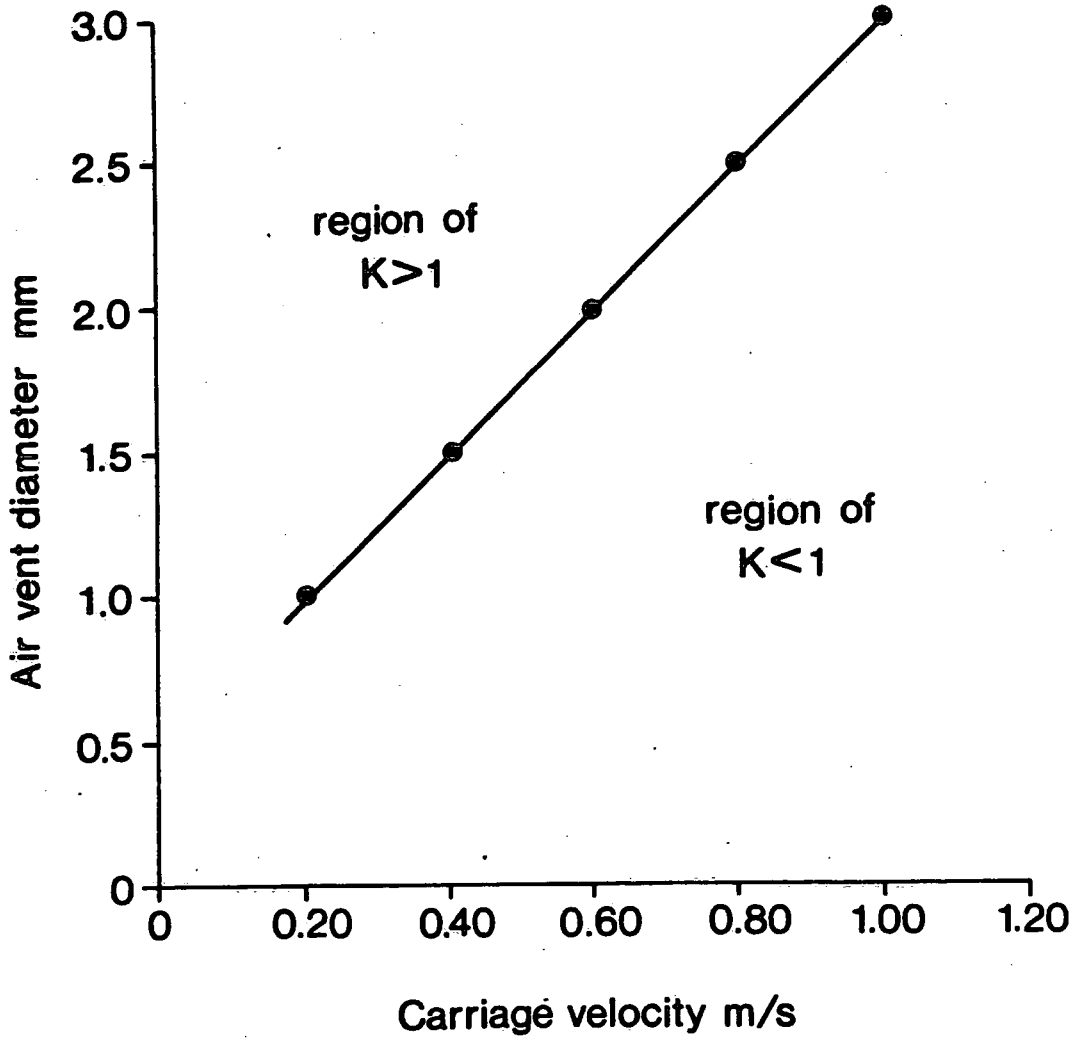

Figure 8 Vent diameter for Iso-kinetic sampling
(ie: $K = V_n / V_s = 1.0$)

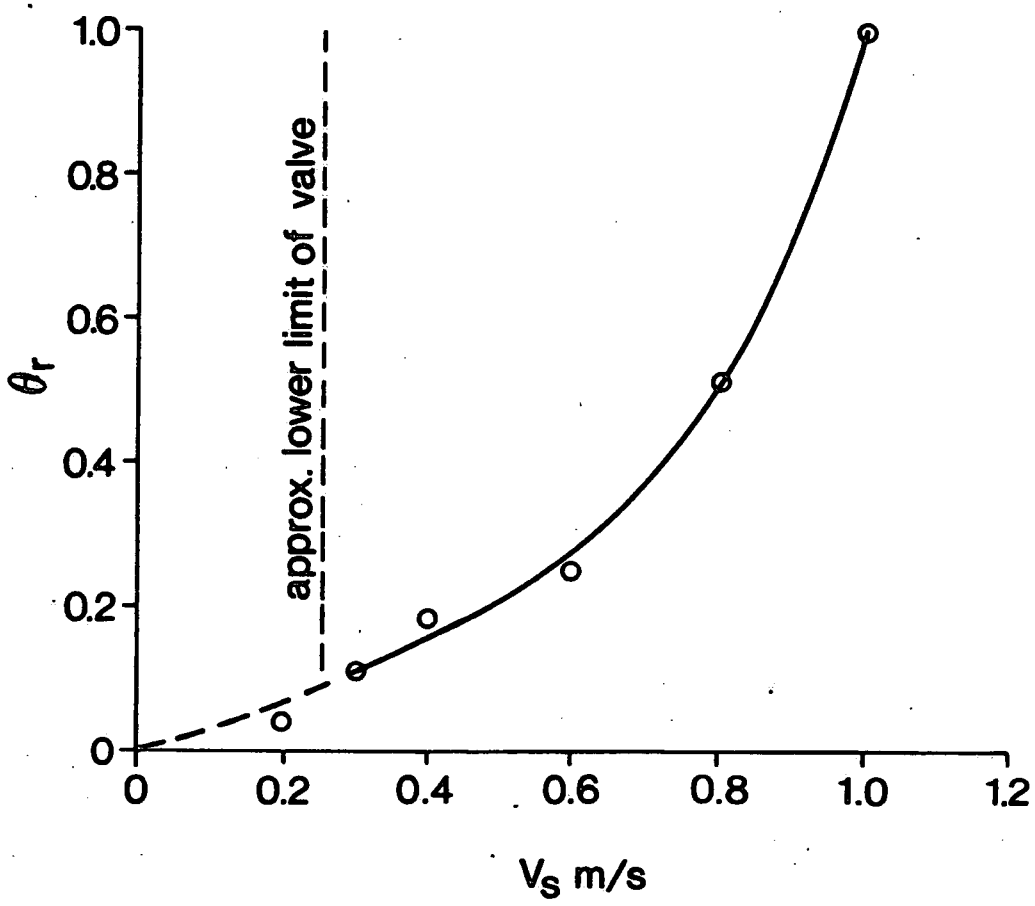

Figure 9 Air valve control curve for DH-81 sampler

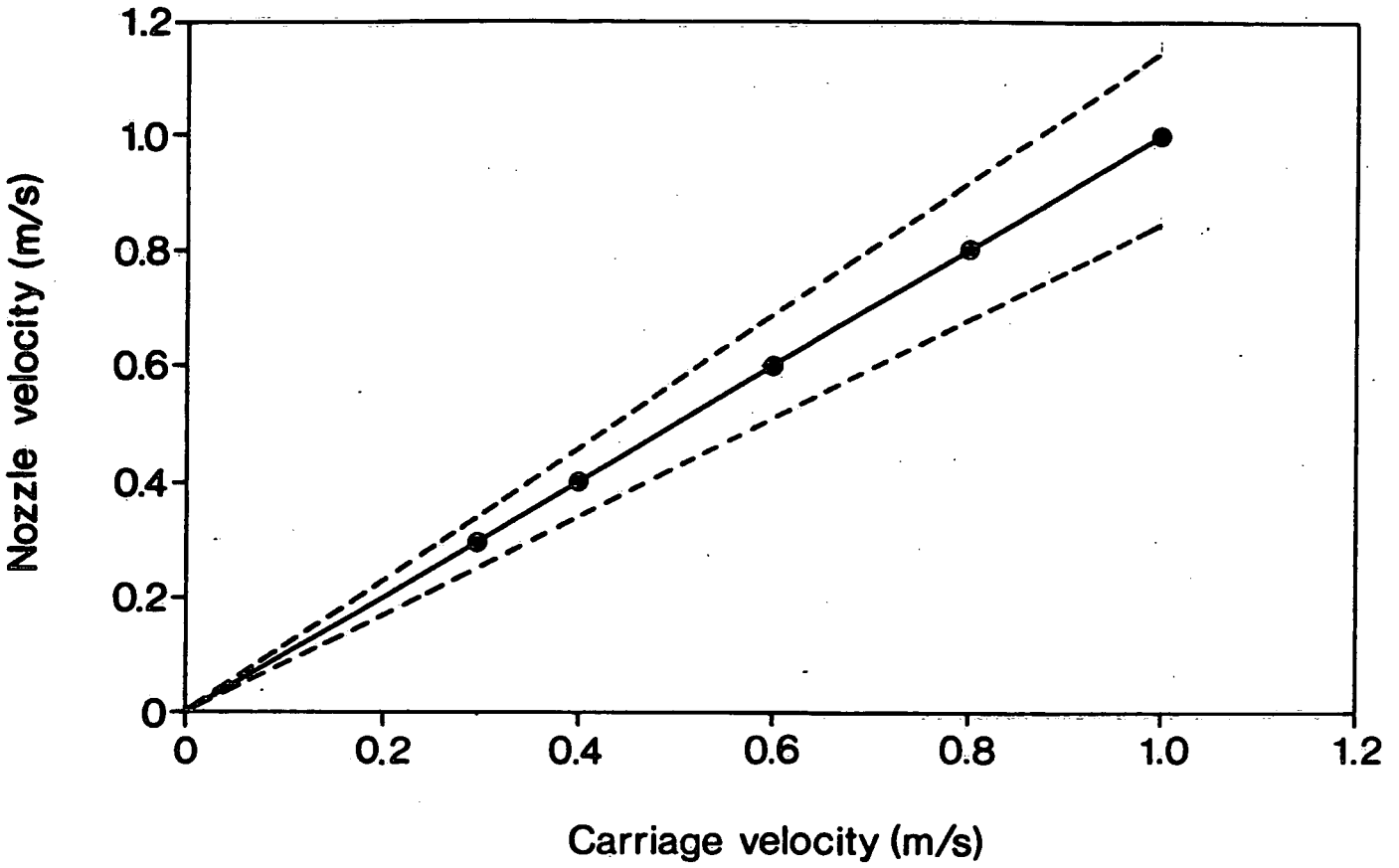

Figure 10 Iso-kinetic sampling for valve control

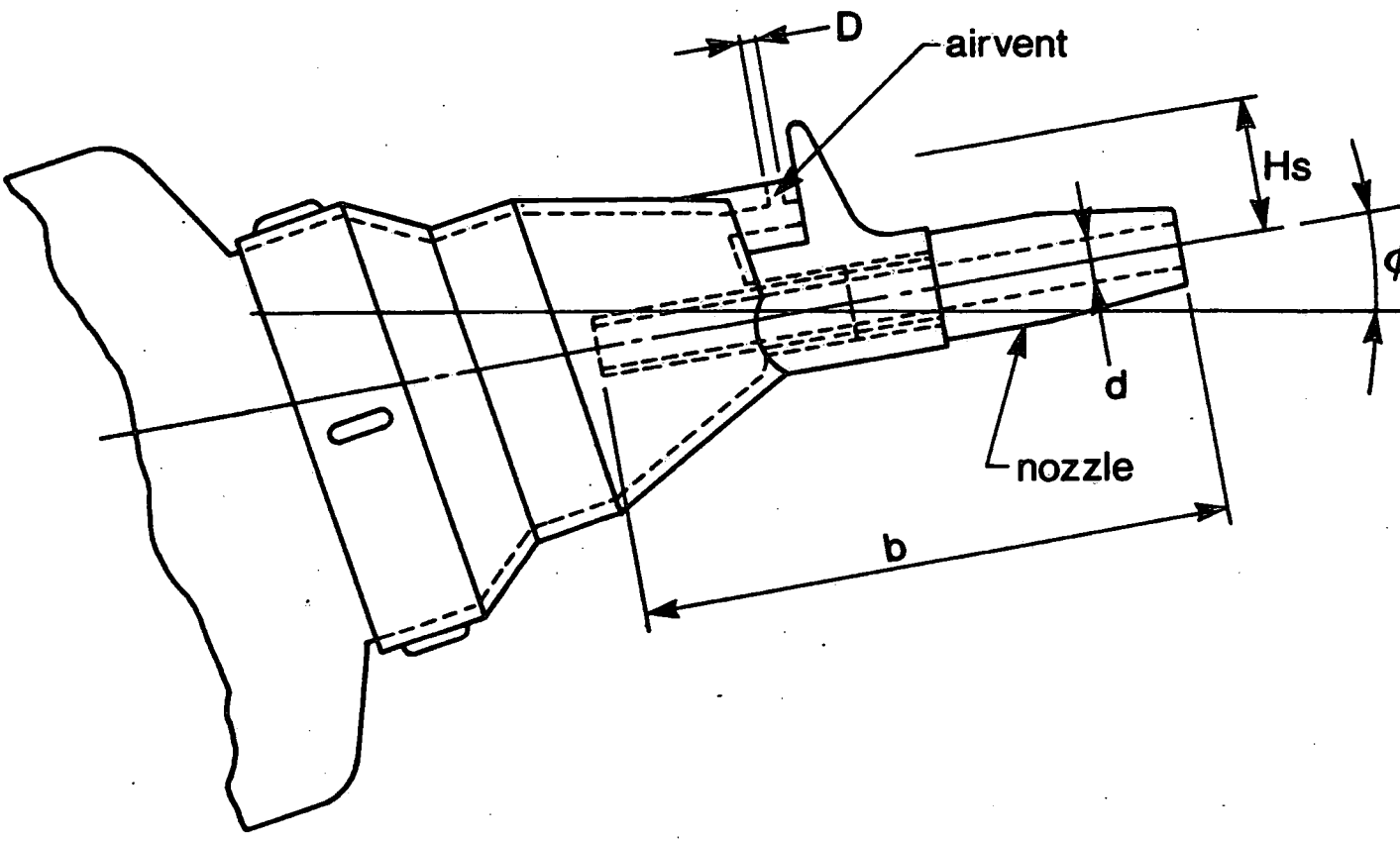

Figure 11 Schematic of DH-81 sampler cap

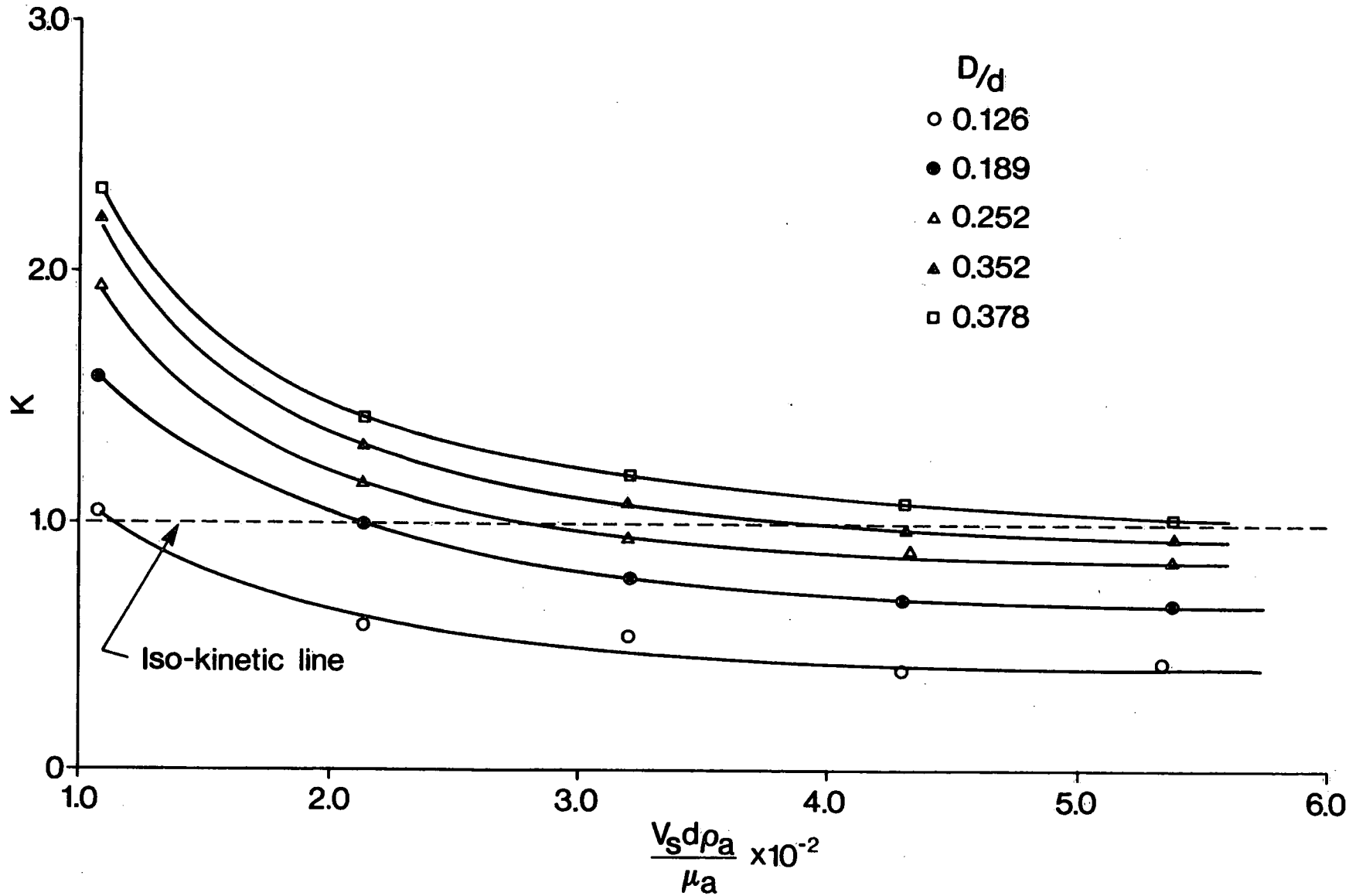

Figure 12 Effect of D/d on performance of sampler

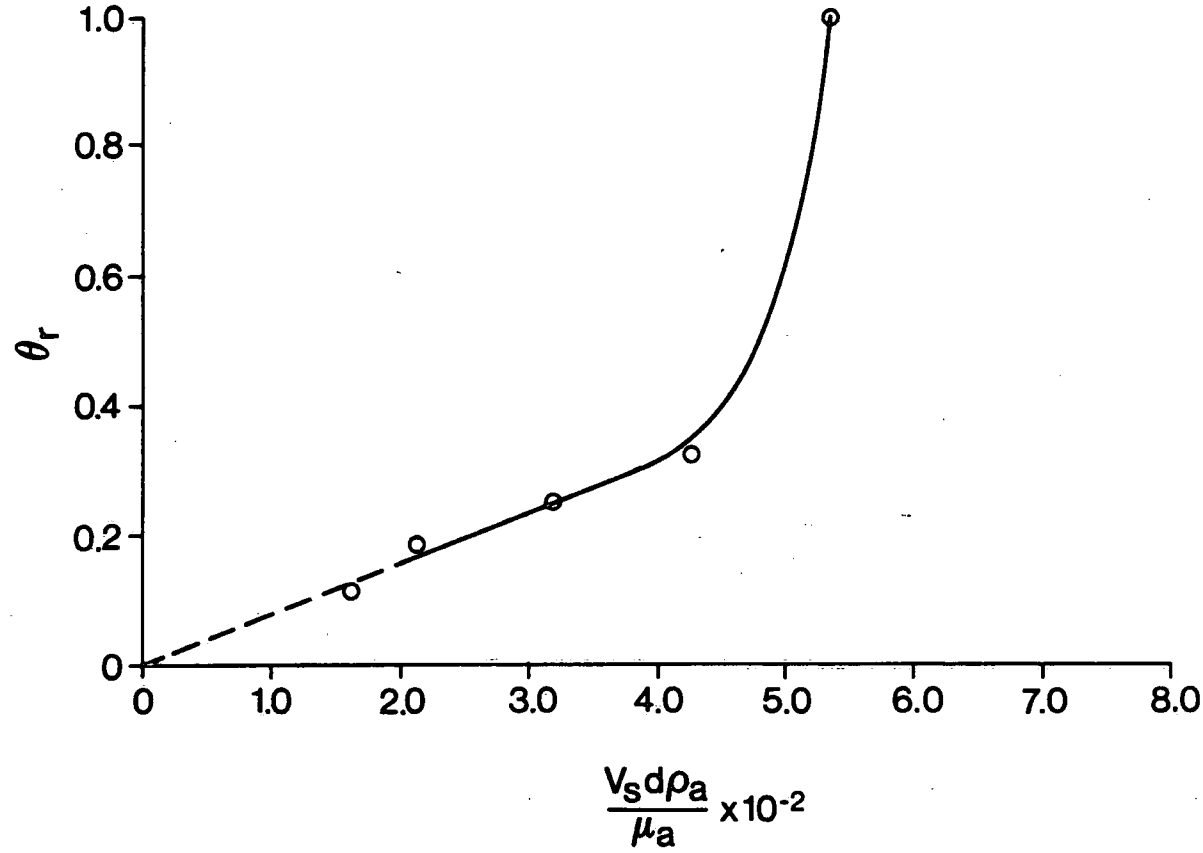

Figure 13 Dimensionless calibration curve for valve control of DH-81 sampler

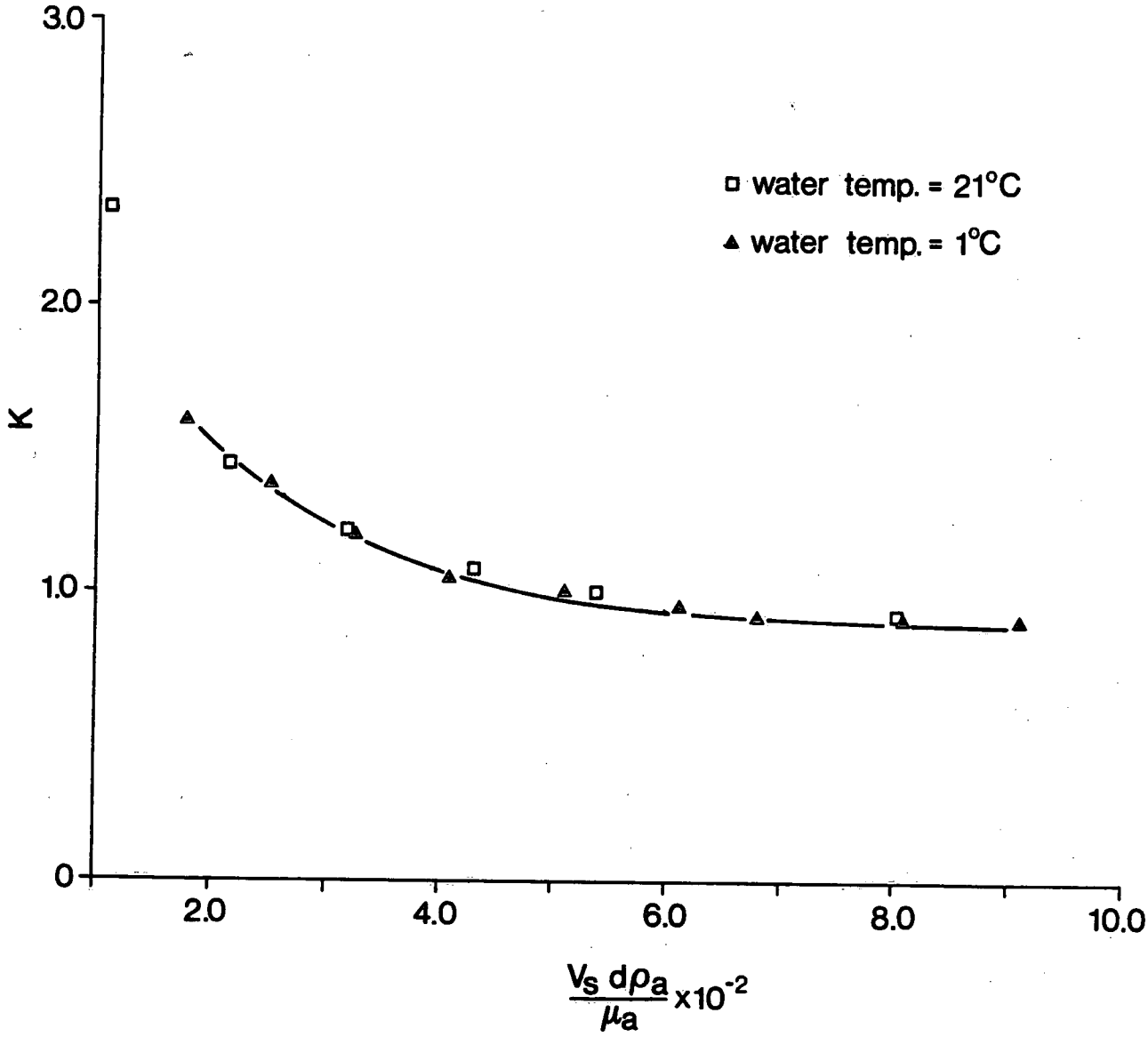

Figure 14 Dimensionless calibration curve

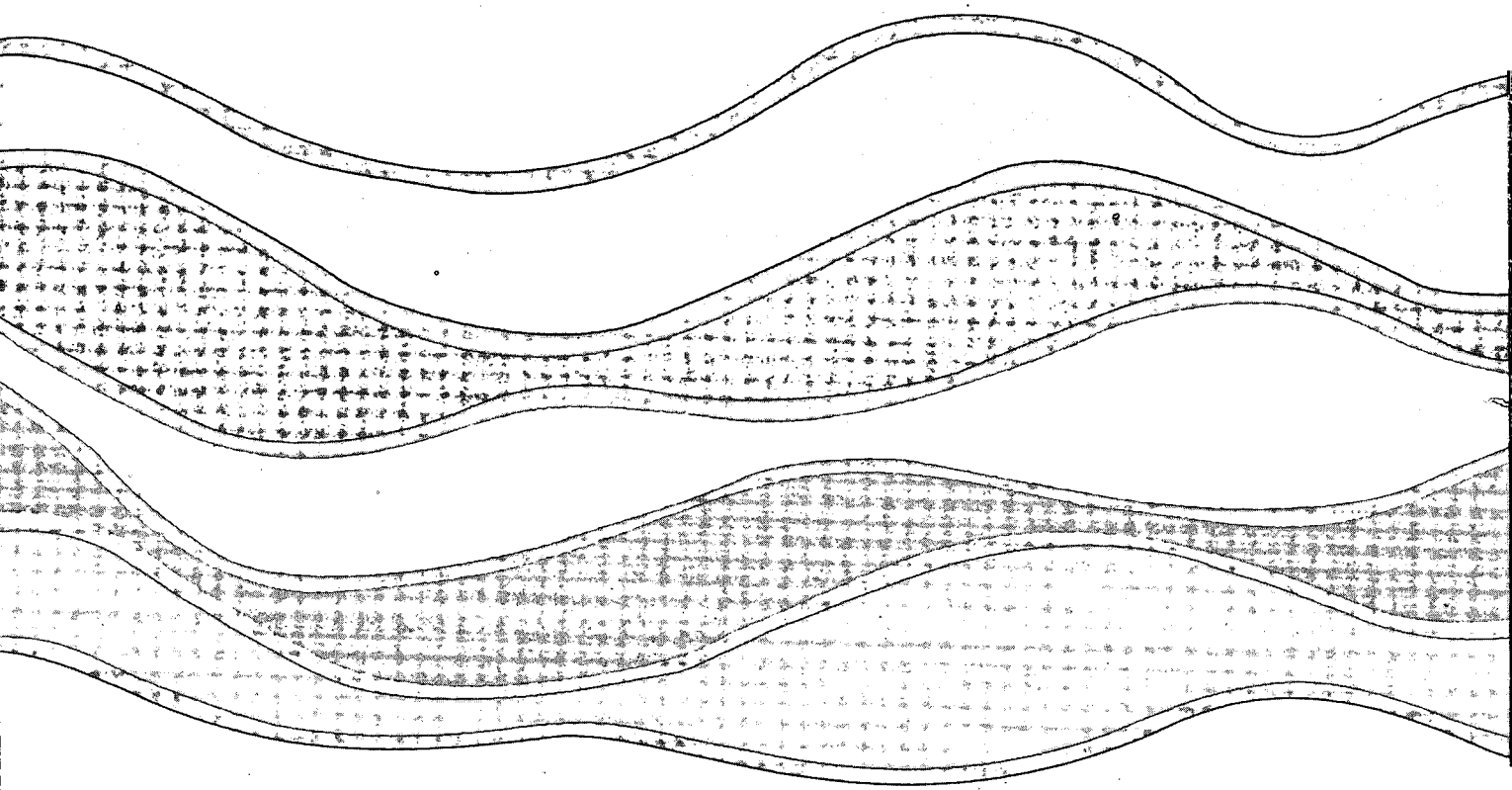

NATIONAL WATER RESEARCH INSTITUTE
P.O. BOX 5050, BURLINGTON, ONTARIO L7R 4A6

Environment Canada Environnement Canada

Canada

INSTITUT NATIONAL DE RECHERCHE SUR LES EAUX
C.P. 5050, BURLINGTON (ONTARIO) L7R 4A6